

Chapter 4 Nadir looking UV measurement.

Part-I: Theory and algorithm

- Aerosol and tropospheric ozone retrieval method using continuous UV spectra -

Atmospheric composition measurements from satellites are essential for monitoring the earth's environment. The instrument discussed here covers from 306 to 452 nm back scattered light with 0.5 nm spectral and 20 km spatial resolution using a Fastie-Ebert type polychromator and a one-dimensional UV Si-CMOS array detector. It is a nadir-looking mapping spectrometer with a mechanical scanner, which can acquire global data in one day. It is expected to provide information about total O₃, SO₂, NO₂, BrO, OClO, HCHO, cloud height, and aerosol characteristics. Total O₃ is inferred from look-up tables calculated with the radiative transfer on multiple solar back scattering. Other constituents are derived in such a way that the deviation of the measured and calculated radiance is minimized.

In recent years, tropospheric O₃ measurement has become important for biomass burning and urban air pollution monitoring. The sensitivity of various O₃ vertical profiles on the measured spectra is studied and tropospheric O₃ retrieval algorithm will be presented. The algorithm studied in this chapter retrieves the geophysical parameters by single instrument without using *a priori* information except for surface albedo.¹

¹ The part of this chapter has been published in "Atmospheric composition measurement from ozone dynamics UV spectrometer (ODUS)," **SPIE 4135**, (2000) and was co-authored by M. Suzuki, and T. Ogawa.

4.1. Objectives

For two decades, total ozone mapping spectrometer (TOMS) instruments have been taking measurements from NIMBUS 7 (1978-1993), METEOR 3 (1991-1994), ADEOS (1996-1997) and Earth Probe (1996-). They have six UV spectral channels with 1 nm spectral resolution [Heath *et al.*, 1975]. NASDA/EORC has developed its own algorithm to retrieve total O₃ and albedo. All ADEOS TOMS data are processed at EORC [Kuze *et al.*, 1998]. TOMS can retrieve the surface albedo and aerosol from 6 channel data. By using 380 nm spectral channel of NIMBUS 7 TOMS, aerosol properties can be retrieved [Torres *et al.*, 1998]. The global ozone monitoring experiment (GOME) onboard the ESA ERS2 has been measuring continuous spectra since 1995 [Burrows *et al.*, 1992]. It has a 0.2 nm spectral resolution with a 40 by 320 km instantaneous field of view (IFOV). It has also retrieved minor constituents such as BrO, OCIO, and HCHO [Chance *et al.*, 1998]. The solar backscattered ultraviolet (SBUV) instruments onboard NIMBUS 7 and NOAA satellites have been providing the stratospheric O₃ profile using 8 spectral channels [Fleig *et al.*, 1990 and Rodgers, 1990]. Total O₃ is estimated using a longer wavelength and then the vertical profile of the stratosphere is retrieved.

The detailed instrument design will be described in Chapter 5. The projected satellite orbit will be 650 km high with a 69 degrees inclination in order to acquire global O₃ data in one day. The specifications of the satellite are summarized in Table 4-1. The UV spectrometer will provide the data for both operational and research purposes. Scientific objectives will be to obtain information on:

- (1) Global total and tropospheric O₃ distribution,
- (2) Dynamics in the stratosphere using O₃ distribution data,
- (3) Pollution source monitoring (oxidation process) (acid deposition: NO₂ and SO₂),
- (4) UV region radiation budget including surface albedo mapping,
- (5) Aerosol optical thickness and spectral characteristics in UV and visible, and,
- (6) Aerosol and cloud height.

The instrument specifications are summarized in Table 4-2. It is a Fastie-Ebert polychromator, which has a uniform slit function in the wide spectral range (300-452 nm). Compared with TOMS, it provides both higher spectral and spatial resolution by replacing the single photo multiplier tube with a linear array solid state detector.

The hybrid CMOS-Si array detector is customized for the UV spectrometer. It has 232 pixels and CMOS amplifiers for 300-452 nm continuous spectral coverage and two additional pixels for offset level monitoring. The thin passivation is carefully designed to maximize the UV quantum efficiency. Each pixel has a different height depending on the cross-dispersion direction image size in order to collect as much input flux as possible. Each pixel is directly connected to its pre amplifier, which is mounted on the same tip and has two gain levels. Thus the array detector design is optimized to achieve high signal-to-noise ratio (SNR). For cloud, aerosol, and surface albedo measurements, it also has higher spatial resolution than the existing instruments.

Table 4-1. Satellite Parameters.

Orbit	Non-sun synchronous (Yaw maneuver)
Altitude	650 km
Inclination	68 deg
Period	98 min

Table 4-2. Specifications of space borne UV spectrometer.

FOV	120 deg
IFOV	1.8 deg (20 km at nadir)
Cross track scan	Stepper motor
Spectral coverage	
Band 1	306- 400 nm
Band 2	432- 452 nm
Band 3	760 nm
Spectral resolution	0.5 nm (sampling interval) 0.6 nm (FWHM)
Spectrometer	Fastie-Ebert polychromator F: 5, focal length: 250 mm
Detector	1 D array 232 spectral channels + 2 offset level monitor
Depolarizer	Calcite (Lyot type)
Solar irradiance measurement	Sand blasted Al (3) Spectralon (1)
Wavelength calibration	Hg lamp

The global total O₃ distribution data acquired in one day will be processed in near real time after the data is down linked to the ground. Research data on minor constituents etc. will be processed separately. For the O₃ profile retrieval of the existing instruments, back-scattered spectra of 250-300 nm, which are mainly scattered in the stratosphere, have been used. For vertical distribution retrieval, the back-scattered spectra of 306-325 nm spectra are mainly used instead of shorter wavelengths. In addition, cloud, aerosol, and minor constituents will be retrieved with a single instrument. The retrieval flow and its accuracy are studied here. Instrumentation will be discuss in Chapter 5. Stratospheric O₃ is inferred by subtracting tropospheric O₃ from the total O₃. Daily stratospheric data will provide information on the dynamics of the stratosphere.

4.2. Radiative Transfer and Retrieval Algorithm

4.2.1. Radiative transfer in UV and visible region

Figure 4-1 schematically illustrates the solar UV radiative transfer in the earth's atmosphere. The

backscattered solar radiation I is divided into two parts as expressed by equation (1): I_a and I_g . I_a is the component that does not reach either the earth's surface or thick cloud tops, while I_g does reach the earth's surface or the cloud tops at least once and is reflected back into space:

$$I = (I_a + I_g) = I_a + \frac{F \cos(\theta)}{\pi} R_s \frac{T_a}{1 - R_s T_b}, \quad (4-1)$$

where F is the solar radiation, θ is the solar zenith angle, R_s is the surface albedo (the reflectivity of the ground or cloud top), T_a is the transmittance by which the radiation reflected by the earth's surface goes through the atmosphere to outer space, and T_b is the ratio at which the reflected radiation is scattered back to the surface.

Both I_a and I_g include multiple scattered radiation.

The earth's albedo R_e is the measured value and defined as the ratio of back scattered radiance and solar irradiance as shown below,

$$R_e = \frac{I\pi}{F \cos(\theta)}. \quad (4-2)$$

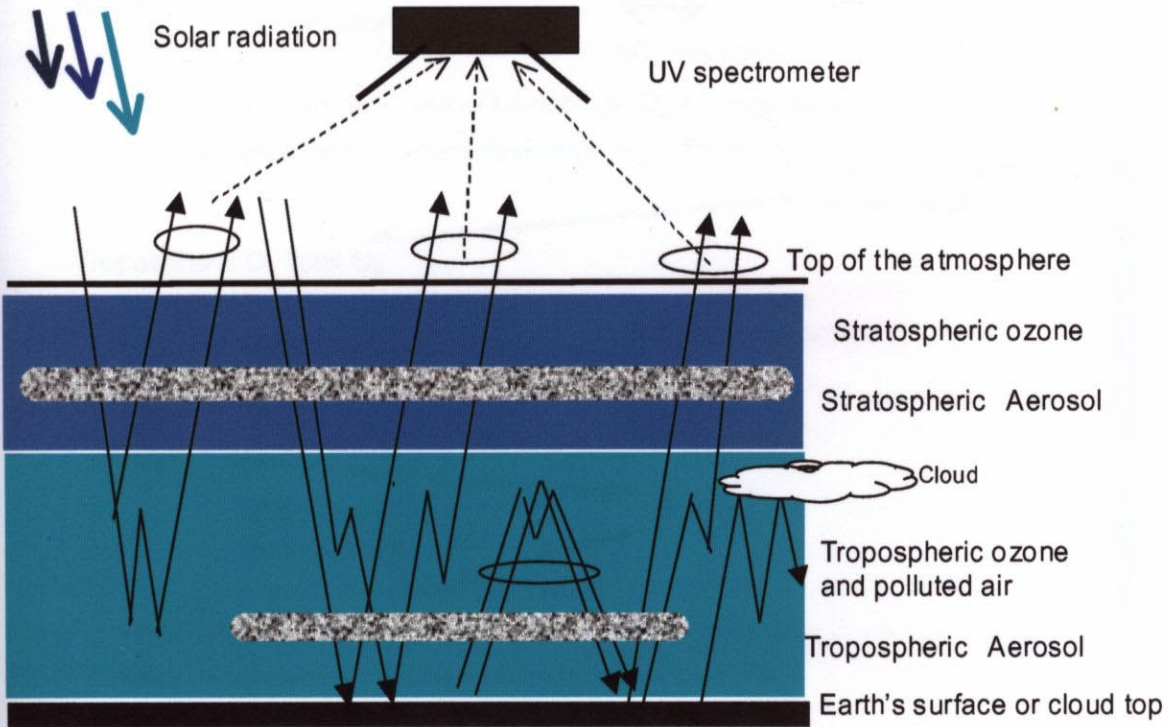


Figure 4-1. Schematics of radiative transfer in the UV and visible region.

4.2.2. Retrieval flow

In this chapter, the retrieval and its output products will be discussed. First, the retrieval flow of TOMS is shown in Figure 4-2. Next the spectral range and the retrieval flow using continuous UV spectra and $O_2 A$ band are summarized in Figure 4-3. Detailed study on retrieving each output products using continuous

spectra is described.

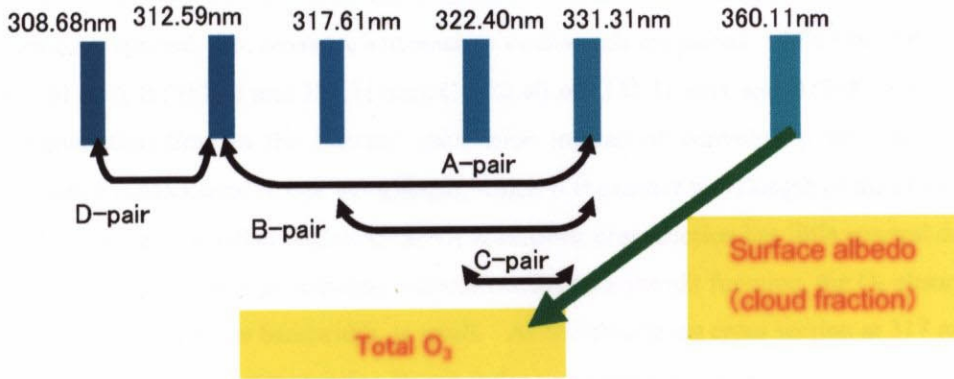


Figure 4-2. The spectral coverage and retrieval flow of TOMS.

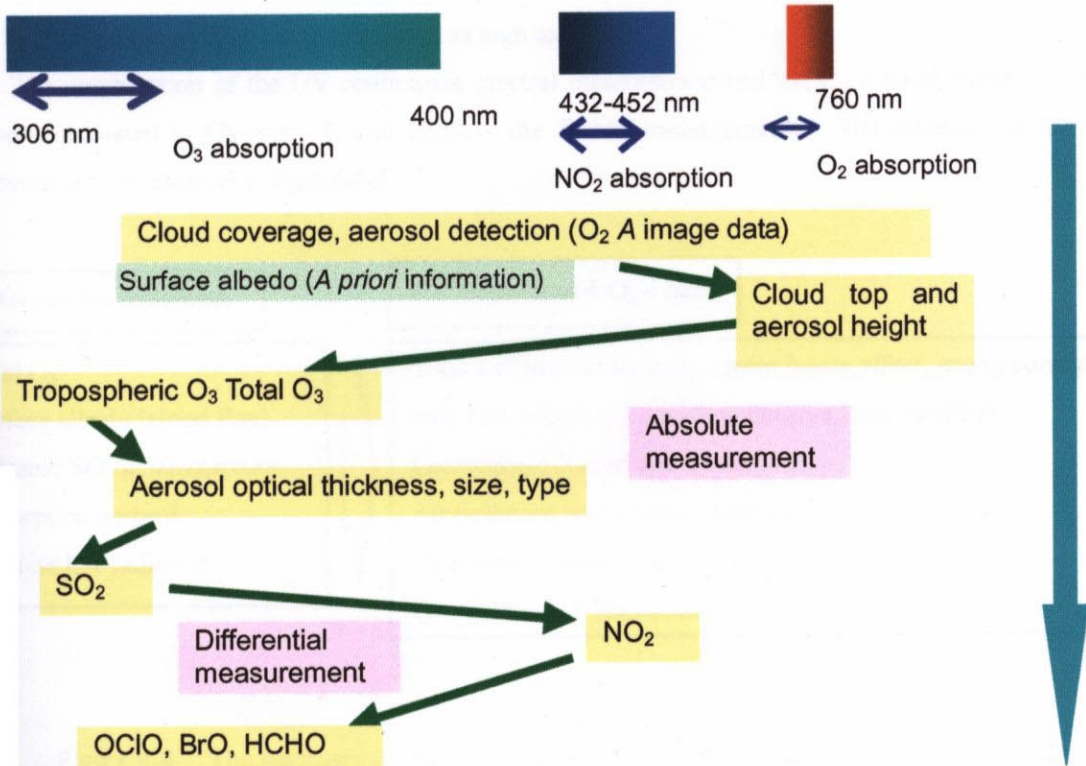


Figure 4-3. Spectral coverage and retrieval flow using the continuous UV spectra and $O_2 A$ band.

4.2.3. TOMS Retrieval and its Error Sources

Before describing the newly developed algorithm, we will discuss the TOMS retrieval and its error source. As the multiple-scattering calculation is time consuming, the look-up tables are prepared before processing the TOMS data. The I_w , $T_{a,}$ and T_b in equation (4-1) are calculated and stored as the look-up tables. The

parameters of the table are the wavelength, solar zenith angles, viewing angles, clouds (cloud-free and clouds existing at an altitude of 0.4 atm), and the total O₃ amount. The total O₃ is retrieved in such a way as to minimize the deviation between the measured and simulated radiance. To reduce the instrument degradation effect, the pair method is applied. O₃ sensitive and insensitive channels are paired. ADEOS/TOMS has 4 pairs, A (312.59 and 331.31 nm), B (317.61 and 331.31 nm), C (322.40 and 331.31 nm), and D (308.68 and 312.59 nm). To reduce the computation time in the forward calculation instead of convoluting the fine spectral step calculation, the radiance is calculated in one wavelength, which is the center wavelength of the channel. When the bandwidth of the channel is small enough and the O₃ absorption cross section has little spectral dependency, the error due to simplifying the spectral response without convoluting the slit function, the O₃ absorption cross section and the solar spectra over the bandwidth, is small. As the absorption cross section at 317 nm has little spectral dependency, the retrieval accuracy using B-pair is the best among the 4 pairs.

The TOMS spectral resolution (the FWHM of the slit function) is 1 nm. It is slightly larger than the spectral structure of the O₃ absorption cross section. The error due to simplifying the spectral response is one of the major error sources in the total O₃ retrieval. The newly designed UV polychromator can minimize this error by making the spectral resolution twice as high as TOMS.

The combination of the UV continuous spectral measurement and the O₂ A band measurement, which has been discussed in Chapter 3, will improve the TOMS measurements. The summary of the expected improvement is illustrated in Figure 4-4

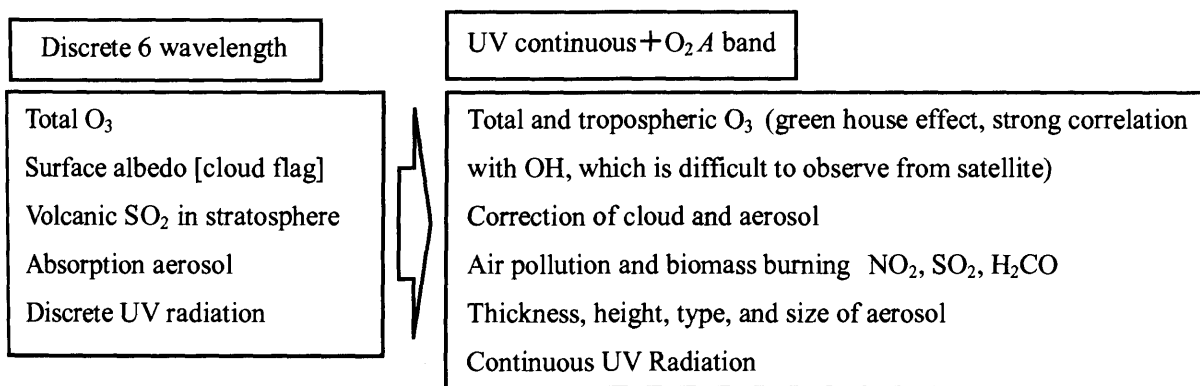


Figure 4-4. The summary of the improvement by the UV continuous spectral and the O₂ A band measurements

4.2.4. Surface Albedo in UV Region

Figure 4-5 is the surface albedo model used in MODTRAN radiative transfer model. The detail spectral information is not included in UV region. However, 14 years NIMBUS 7 TOMS has provided the global surface albedo dataset at 380 nm as shown in Figure 4-6. The data shows both land and ocean surface albedo is very low except for the ice surface in high latitude and the measured spectra from space are less affected by the earth surface than other spectral region. These characteristics are important for atmosphere

observation.

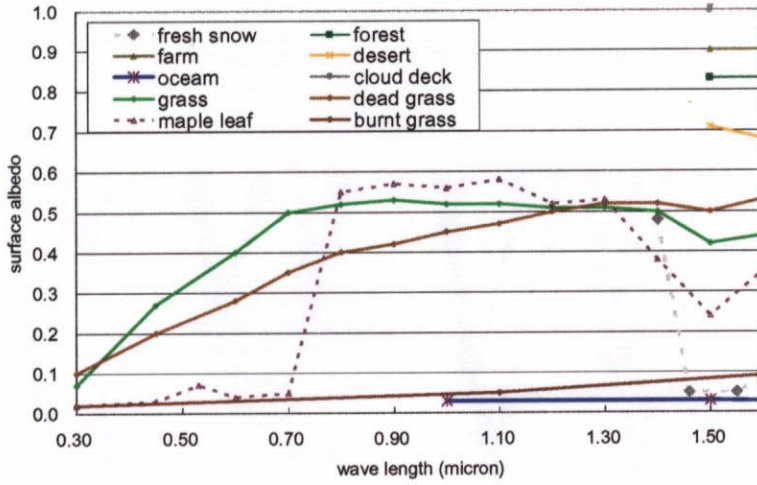


Figure 4-5. Spectral characteristics model of the surface albedo of MODTRAN.

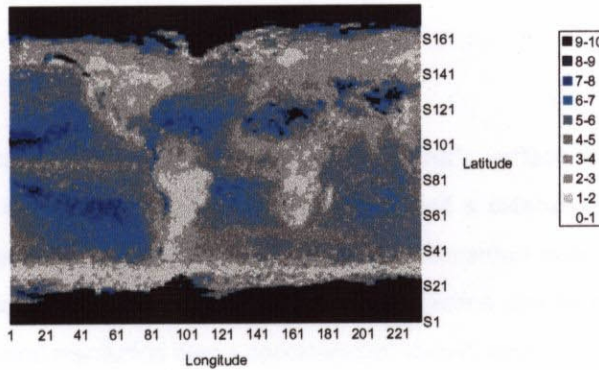


Figure 4-6. Lambert albedo annual minima of 380 nm in % measured with NIMBUS 7 TOMS.

4.3. Cloud and Aerosol Effects

4.3.1. Scenario

Table 4-3 indicates the scenarios of cloud and aerosol detection. The clear sky and partial clouds of scenarios 1 and 4 are easily detected with an imager or radiometer with a two-dimensional array detector. Scenarios 2 and 3 are discussed in this section using the $O_2 A$ band spectroscopy application. Figure 4-7 schematically illustrates the radiative transfer in the UV region in presence of clouds and aerosols.

Table 4-3. Scenarios of cloud and aerosol detection.

Scenario 1	Clear within in pixel
Scenario 2	Fully covered with aerosol
Scenario 3	Fully covered with cirrus and lower altitude thick cloud
Scenario 4	Partially covered with thick cloud within pixel

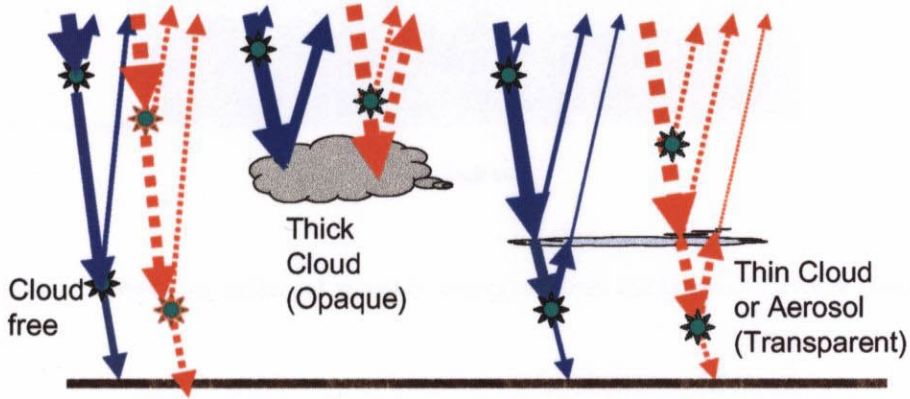


Figure 4-7. Radiative transfer in UV region in case of cloud and aerosol: (a) shorter wavelength (solid line) and (b) longer wavelength (dotted line).

4.3.2. Cloud Coverage

(1) Cloud database

Recent satellite observation indicated that most of the Earth's surface is covered by clouds. The International Satellite Cloud Climatology Project (ISCCP) provided a database on various types of clouds amounts, as illustrated in Figure 4-8. However, this statistical information is not sufficient for the accurate retrieval of the total O_3 . Cloud information such as the cloud fraction and height must be retrieved. An imager, which has greater spectral resolution than a spectrometer, should ideally be borne on the same platform to provide cloud fraction information simultaneously by viewing the same IFOV. Moreover the cloud fraction information alone is only is not sufficient. Terra MODIS can measure thin clouds with optical thickness as low as 0.02 and provide cloud thickness data [Dessler and Yang, 2003]. Most cirrus clouds have an optical thickness of less than 0.04. The impact of cirrus cloud on effective air-mass factor will be discussed in this chapter.

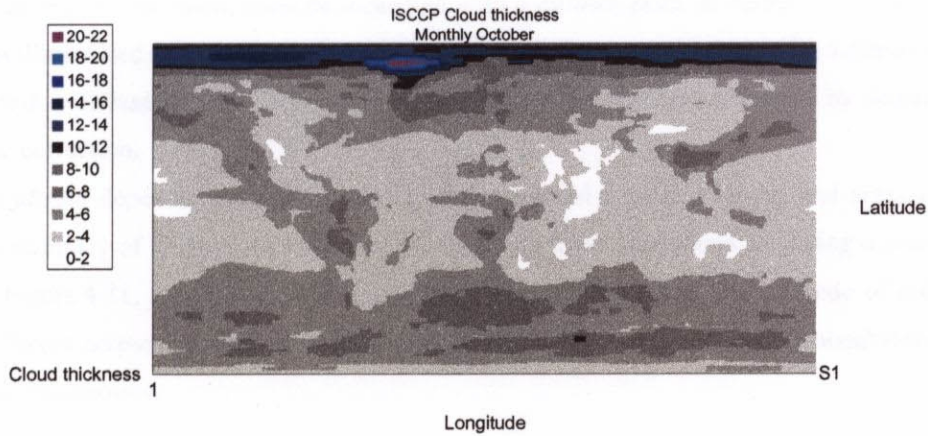


Figure 4-8. Global distribution of monthly averaged cloud thickness of October from ISCCP database.

(2) Cloud size distribution

Few databases on the cloud horizontal size distribution are available [Houze, 1993]. Figure 4-9 provides cloud size distribution statistical data acquired from geostationary satellites. The data indicates that 90 % of clouds have a size between 10^2 and 10^4 km². Therefore, the possibility of avoiding cloud contamination is increased if the IFOV is less than 10 km.

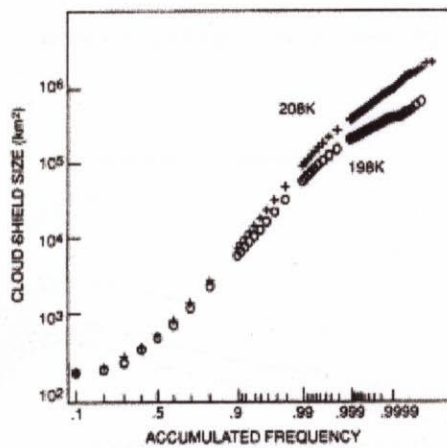


Figure 4-9. Cloud size distribution of low latitudes based on the geostationary satellite IR imager data.

4.3.3. Earth's Albedo in the UV region

(1) Forward calculation

A UV polychromator measures Earth's albedo as defined in equations (4-1) and (4-2). Earth's albedo is the index of Earth's atmospheric radiation budget in the UV and visible regions. Solar irradiance, as well as

scattered radiance from the nadir, must be measured with a diffuser plate on board. The instrument has four diffuser plates illuminated by direct solar flux: three sand-blasted-aluminum plates with different exposure times and one spectralon diffuser plate. This combination will minimize the errors caused by degradation onboard and geometric correction.

Earth's albedo depends on cloud type and height, aerosol type and height, and surface albedo. The measurement accuracy of O_3 is much improved by retrieving these parameters and using *a priori* information. Figure 4-10, Figure 4-11, Figure 4-12, and Figure 4-13 respectively depict Earth albedo of different types of clouds; of different aerosol models; of surface albedos of 0, 0.05, and 0.10; and of nonabsorbent aerosols of various optical thicknesses.

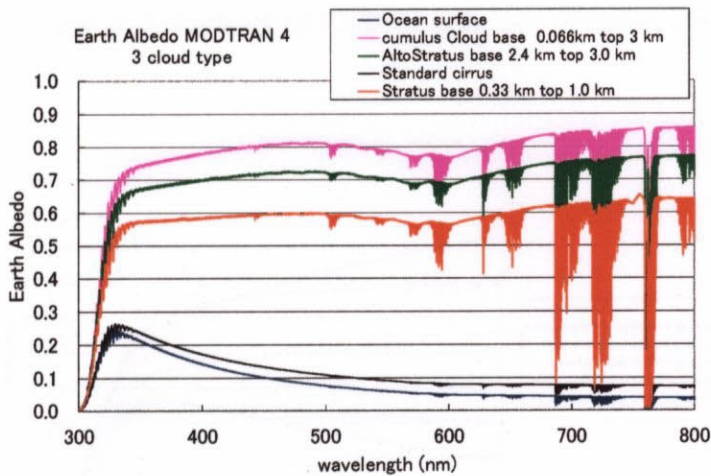


Figure 4-10. Simulated earth albedo of different type of clouds by MODTRAN4.

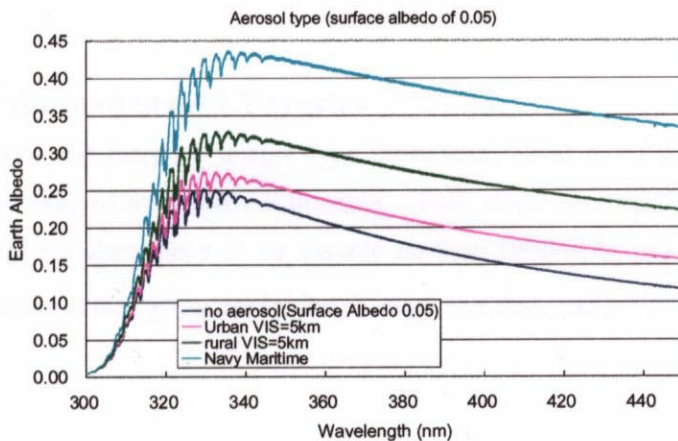


Figure 4-11. Simulated spectral radiance in the case of different aerosol models of MODTRAN4.

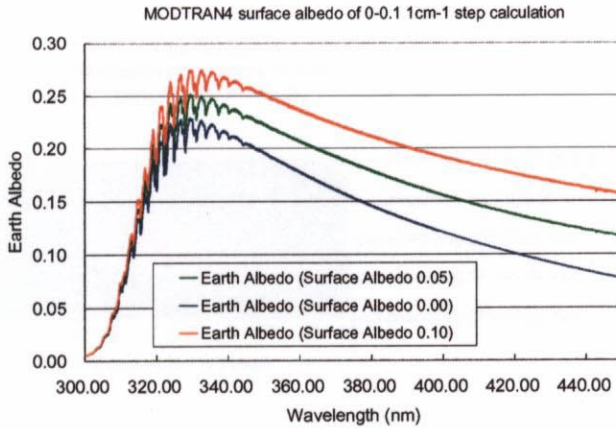


Figure 4-12. Simulated earth albedo by MODTRAN in the case of surface albedo of 0, 0.05, and 0.10.

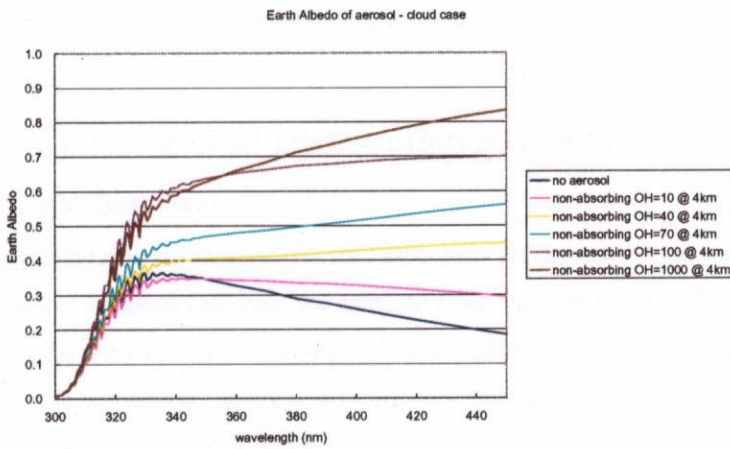


Figure 4-13. Simulated earth albedo for of non-absorbing aerosol of various optical thickness.

(2) Retrieval using the continuous UV spectra

If the satellite does not carry an imager type instrument, cloud coverage must be retrieved using continuous spectra data obtained by a single instrument. Both cloud coverage and optical thickness (thick clouds) can be retrieved simultaneously if we assume uniform reflectivity (no absorption). Figure 4-14 depicts the simulated results of the χ^2 variation for coverage and thickness retrieval of clouds.

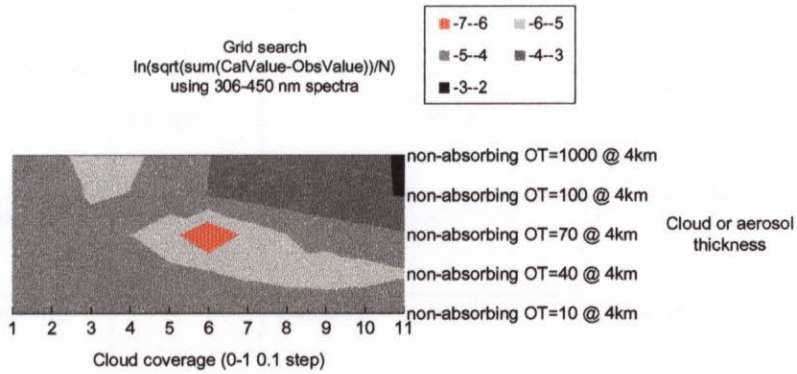


Figure 4-14. The sum of the earth's albedo deviation at whole spectra region, which is minimized in the fitting process to determine the cloud coverage and thickness.

4.4. Aerosol and Cloud Vertical Distribution Retrieval

4.4.1. Cloud Top Height Retrieval

Clouds play an important role in radiative transfer, especially for the total O_3 measurement, because the O_3 existing below clouds cannot be observed from the satellite orbit. In the ADEOS/TOMS retrieval, the cloud coverage is inferred from the retrieved surface albedo. If it is higher than 0.6, the scene is assumed to be fully covered with clouds. If it is between 0.2 and 0.6, it is assumed that the IFOV is partially covered with clouds. In addition, clouds are assumed to exist at the altitude level of 0.4 atm. The effective optical path length must be measured to improve the accuracy of the total O_3 and tropospheric O_3 measurements. Several cloud detection methods are compared and summarized in Table 4-4. $O_2 A$ band absorption is applied for cloud detection as discussed in Chapter 3. Filter radiometers are installed in addition to the main UV grating spectrometer. They determine the distance between cloud tops and the satellite from the optical thickness of $O_2 A$ band absorption. Cloud coverage and its top height can be simultaneously estimated using three channels (O_2 weak, strong and no absorption), which estimate the cloud top height with accuracy better than 1 km. Another method uses the ring effect of the Fraunhofer spectra around 390 nm [Joiner *et al.*, 1995 and Chance *et al.*, 1997]. This method requires extremely high spectral resolution and SNR. A thermal infrared imager also can provide cloud-height information. However, temperature vertical profile must be modeled. The CO_2 slicing method can provide more accurate cloud-height information than a thermal imager, but a complicated thermal infrared instrument is required [Smith and Platt, 1978].

Table 4-4. Comparison of cloud detection methods.

Method	O ₂ A band	Visible Imager	IR Imager	CO ₂ slicing (IR)	Ring Effect (UV)	Polarization	H ₂ O absorption (SWIR)
Cloud coverage	possible	possible	possible	-	-	-	-
Cloud height	possible	-	possible	possible	possible	-	-
Thin cloud	possible	-	-	possible	-	-	-
Application	GOME	Weather satellite	Weather satellite	NIMBUS	SBUV GOME	GOME	-

Figure 4-15 depicts simulated differential absorption of cloud top heights of 5 km and 2 km for a cloud surface albedo of 0.8. Using the differential absorption spectra of O₂ A band absorption greatly improves the cloud detection accuracy compared with TOMS absolute radiance measurements since the differential absorption is insensitive to any response degradation of the instruments or polarization sensitivity. The instrument discussed in Chapter 5 has a filter radiometer which has three channels in O₂ A band region, at 755 nm (no absorption), 771 nm (weak absorption), and 765 nm (moderate absorption).

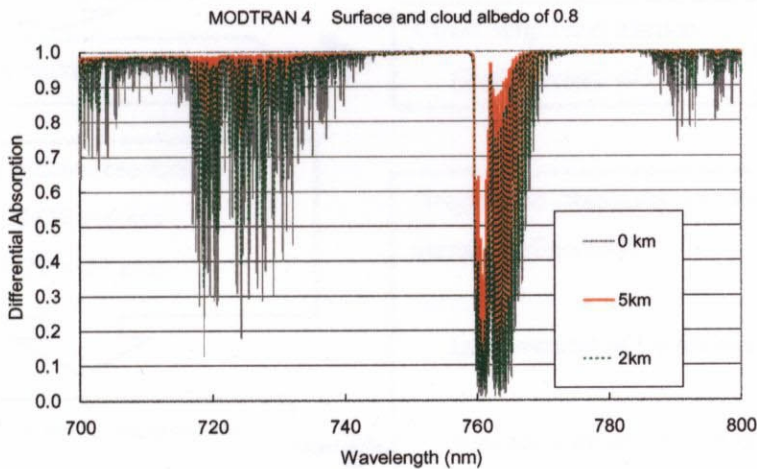


Figure 4-15. Simulated differential absorption of cloud top height of 5 km and 2 km in the case of cloud surface albedo of 0.8.

4.4.2. O₂ A Band Multichannel Spectroscopy

The O₂ A band can be widely used for cloud and aerosol correction because the O₂ profiles are well known and the instrument is not so complicated, as discussed in Chapter 3. Figure 4-16 schematically illustrates the application of O₂ A band multichannel spectroscopy. Selecting the appropriate field of view, which minimizes the frequency of cloud contamination, reveals that the O₂ A band spectra contains the

information regarding thin cloud and aerosol characteristics. The sensitivity and retrieval of the geophysical parameters using the $O_2 A$ band observations are discussed in this section. The absorption convoluted by the instrument function of the moderate spectral resolution channel can be simply expressed to the first order by the exponential function. A moderate combination of the spectral band and optical thickness is discussed here. In addition, a robust algorithm is discussed to minimize the effect of degradation of radiometric accuracy on board during a mission.

Three types of measurements can be applied, as illustrated in Table 4-5. The first simultaneously retrieve cloud fraction and cloud top height. Both cloud coverage and cloud height can be well retrieved by using many spectral channels with different optical thicknesses, as discussed in Chapter 3. The estimated values are 0.6 and 2 km if the assumed surface albedo has a 10 % error, which is one of the worst cases, and the true value of the cloud coverage and top height are 0.5 and 6 km,. The cloud must be sufficiently thick in this example. In contrast, an imager or an $O_2 A$ band radiometer with a two-dimensional array detector, which has greater spatial resolution than a UV spectrometer, the can detect cloud portion directly. Therefore, we use the $O_2 A$ band multichannel information for cloud characteristic retrieval. The algorithm discussed here is utilized to investigate aerosol and thin-cloud characteristics using two different optical thicknesses.

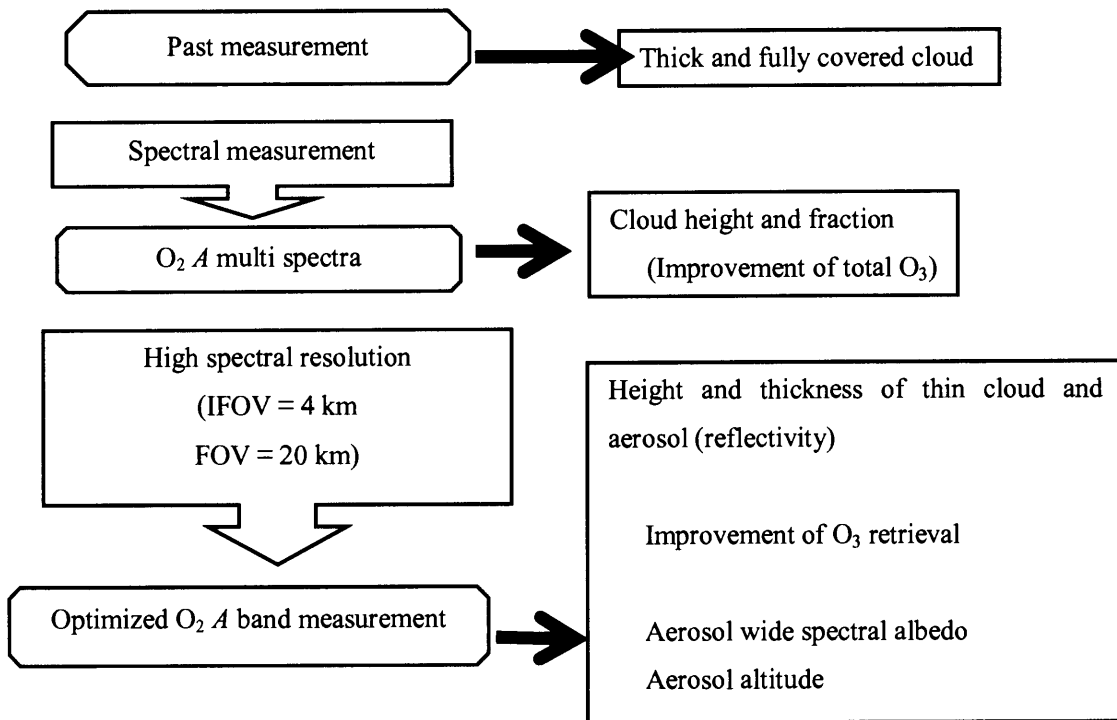


Figure 4-16. The application of $O_2 A$ band multi-channel spectroscopy.

Table 4-5. The application of the O₂ A band multi channel spectroscopy.

	Parameters to be retrieved	Parameters that have to be modeled
Thick cloud top height	Cloud fraction and cloud top height	Surface albedo
Aerosol (Scenario 2)	Aerosol and thin cloud height and their optical thickness	Surface albedo
Thin high altitude cloud (Scenario 3)	Cloud heights of both upper thin cloud and lower thick cloud	Thin cloud optical thickness

(1) Simplified model for O₂ A band absorption

A filter radiometer is an optimized method for O₂ A band measurement, as discussed in Chapter 3. The observed value will become the convolution of the instrument function and absorption spectra and can be simulated as in Figure 4-17. The convoluted absorption spectra can be modeled as an exponential function as illustrated in Figure 4-18. The sensitivity will be studied here using a simplified exponential function.

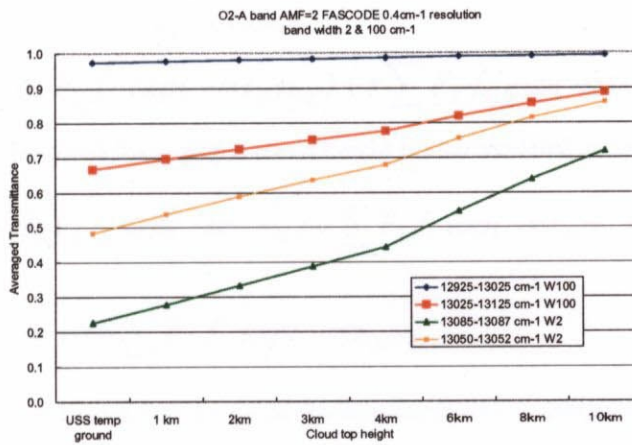


Figure 4-17. Convolutions of the instrument function and the atmospheric transmittance) for O₂ A band channels with center positions of (top to bottom) for instrument resolution $\Delta\gamma = 2.0$ and 100 cm^{-1} .

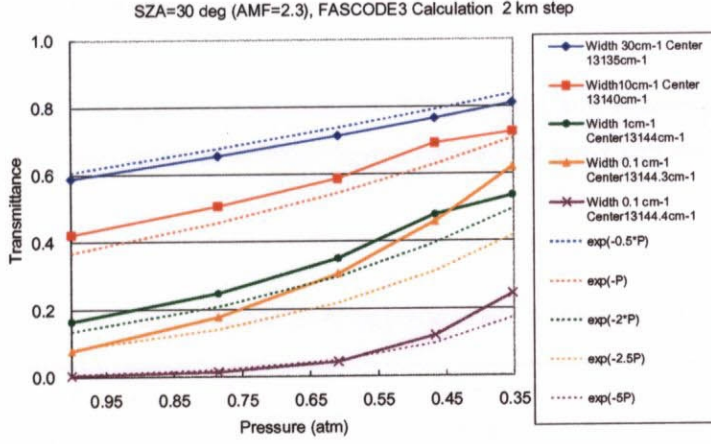


Figure 4-18. Transmittance of various wavelength center and band width of $O_2 A$ band channels and exponential function models as the function of the cloud top height pressure.

(2) Simplified model for a sensitivity study of $O_2 A$ band multi channel observation

Scenarios 1 and 4. The measured spectral radiance can be described as follows, assuming the cloud is thick and the reflectivity of thick cloud is known.

$$I_{\lambda h} = (1-r) \sum \beta_{\lambda} F_{\lambda} f_{\lambda} \exp(-s\alpha_{i\lambda} n_{i0}) + r \sum F_{\lambda} f_{\lambda} \exp(-s\alpha_{i\lambda} n_{ih}). \quad (4-3)$$

The sensitivity to the cloud fraction and cloud height is also modeled as follows.

$$\frac{\partial I_{\lambda h}}{\partial r} = \sum \beta_{\lambda} F_{\lambda} f_{\lambda} \exp(-s\alpha_{i\lambda} n_{ih}) - \sum F_{\lambda} f_{\lambda} \exp(-s\alpha_{i\lambda} n_{i0}),$$

$$\frac{\partial I_{\lambda h}}{\partial h} = s\alpha R \sum F_{\lambda} f_{\lambda} \exp(-s\alpha_{i\lambda} n_{ih}). \quad (4-4)$$

The above equation indicates that the cloud fraction sensitivity is maximized when the cloud top is high. If the cloud height is between 0.2 and 1 atm, then the difference between the O_2 absorption of 0.2 atm and 1 atm must be maximized to maximize the sensitivity to the cloud-height retrieval.

Scenario 2. The measured Earth albedo can be described as follows if the forward scattering of the aerosol and thin cloud is dominant and the field of view is fully covered with the thin cloud or aerosol.

$$I_{\lambda h} = (1-R)^2 \sum \beta_{\lambda} F_{\lambda} f_{\lambda} \frac{\exp(-s\alpha_{i\lambda} n_{ih})}{1 - \beta_{\lambda} R \exp(-s\alpha_{i\lambda} (n_{i0} - n_{ih}))} + R \sum F_{\lambda} f_{\lambda} \exp(-s\alpha_{i\lambda} n_{ih}). \quad (4-5)$$

Scenario 3. The measured Earth albedo can be described as follows if two cloud layers exit and higher cloud is thin and its reflectivity is known.

$$I_{\lambda h} = (1-R_{high})^2 \sum R_{low} F_{\lambda} f_{\lambda} \frac{\exp(-s\alpha_{i\lambda} n_{ih})}{1 - R_{high} R_{low} \exp(-s\alpha_{i\lambda} (n_{ilow} - n_{ihigh}))} + R_{high} \sum F_{\lambda} f_{\lambda} \exp(-s\alpha_{i\lambda} n_{ihigh}). \quad (4-6)$$

The sensitivity is studied in the following section, and the retrieval algorithm is discussed using the simplified model described above.